The EMBO Journal (2007) 26, 690–700 | © 2007 European Molecular Biology Organization | All Rights Reserved 0261-4189/07
www.embojournal.org

THE EMBO JOURNAL

Rgs1 regulates multiple Gα subunits in *Magnaporthe* pathogenesis, asexual growth and thigmotropism

Hao Liu[1], Angayarkanni Suresh[1], Francis S Willard[2], David P Siderovski[2], Shen Lu[3] and Naweed I Naqvi[1,4,*]

[1]Fungal Patho-Biology Group, Temasek Life Sciences Laboratory, National University of Singapore, Singapore, [2]Department of Pharmacology, University of North Carolina, Chapel Hill, NC, USA, [3]Institute of Materials Research and Engineering, Singapore and [4]Department of Biological Sciences, National University of Singapore, Singapore

Regulators of G-protein signaling (RGS proteins) negatively regulate heterotrimeric G-protein cascades that enable eukaryotic cells to perceive and respond to external stimuli. The rice-blast fungus *Magnaporthe grisea* forms specialized infection structures called appressoria in response to inductive surface cues. We isolated *Magnaporthe RGS1* in a screen for mutants that form precocious appressoria on non-inductive surfaces. We report that a thigmotropic cue is necessary for initiating appressoria and for accumulating cAMP. Similar to an *RGS1*-deletion strain, $magA^{G187S}$ (RGS-insensitive $G\alpha_s$) and $magA^{Q208L}$ (GTPase-dead) mutants accumulated excessive cAMP and elaborated appressoria on non-inductive surfaces, suggesting that Rgs1 regulates MagA during pathogenesis. Rgs1 was also found to negatively regulate the $G\alpha_i$ subunit MagB during asexual development. Deficiency of *MAGB* suppressed the hyper-conidiation defect in *RGS1*-deletion strain, whereas $magB^{G183S}$ and $magB^{Q204L}$ mutants produced more conidia, similar to the *RGS1*-deletion strain. Rgs1 physically interacted with GDP·AlF_4^--activated forms of MagA, MagB and MagC (a $G\alpha_{II}$ subunit). Thus, Rgs1 serves as a negative regulator of all Gα subunits in *Magnaporthe* and controls important developmental events during asexual and pathogenic development.

The EMBO Journal (2007) **26,** 690–700. doi:10.1038/sj.emboj.7601536; Published online 25 January 2007
Subject Categories: signal transduction; microbiology & pathogens
Keywords: fungal pathogenesis; G-proteins; *Magnaporthe*; RGS proteins; thigmotropism

Introduction

Heterotrimeric (αβγ) guanine-nucleotide binding proteins (G-proteins) are activated by the seven transmembrane spanning family of receptors (Malbon, 2005). Binding of agonists, such as chemo-attractants, neurotransmitters, hormones, odorants and taste ligands, to such receptors promotes exchange of GDP to GTP on Gα and leads to the dissociation of Gα from the Gβγ heterodimer (Dohlman and Thorner, 2001). Either Gα or Gβγ, or both are then free to activate downstream effectors (Dohlman and Thorner, 2001). Signaling persists until GTP is hydrolyzed owing to the intrinsic GTPase activity of Gα and consequently the GDP-Gα and Gβγ reassociate. Hence, duration of G-protein signaling is controlled by the guanine nucleotide state of Gα (Dohlman and Thorner, 2001). Members of the RGS protein family share a conserved domain of ~120 amino acids and function as key negative regulators of G-protein signaling pathways (Dohlman *et al*, 1996; Koelle and Horvitz, 1996; Siderovski *et al*, 1996). RGS proteins function primarily as GTPase accelerating proteins (GAPs) and increase the hydrolysis rate of GTP bound to the Gα subunits (Siderovski and Willard, 2005). Structures of the $G_{i\alpha1}$–GDP–AlF_4^-–RGS4 and $G\alpha_t$–GDP–AlF_4^-–RGS9 complexes revealed that RGS proteins exert their GAP activity primarily by stabilizing the transition state for GTP hydrolysis (Tesmer *et al*, 1997a; Slep *et al*, 2001). Based on sequence similarity and biological properties, 16 distinct mammalian Gα subunits have been classified into four families: $G\alpha_s$, $G\alpha_i$, $G\alpha_q$ and $G\alpha_{12/13}$ (Fukuhara *et al*, 2001). To date, RGS proteins have been definitively shown to regulate $G\alpha_i$, $G\alpha_q$ and $G\alpha_{12/13}$, but it is controversial as to whether a bona fide GAP exists for a $G\alpha_s$ subunit (Zheng *et al*, 2001; Castellone *et al*, 2005).

G-protein-mediated signaling is one of the most important mechanisms by which eukaryotic cells sense extracellular signals and integrate them into intrinsic signal transduction pathways. In fungi, G-proteins are involved in the regulation of a variety of cellular functions in vegetative growth and/or pathogenic development, such as conidiation, infection structure differentiation and pathogenicity (Bolker, 1998; Lengeler *et al*, 2000; Yu, 2006).

The filamentous ascomycete *Magnaporthe grisea* causes the devastating rice-blast disease (Ou, 1985). The appressorium, a unicellular infection structure employed by *M. grisea* to breach the plant surface, is elaborated by a conidium at the tip of a germ tube in response to specific environmental and physicochemical surface signals (Lee and Dean, 1993; Gilbert *et al*, 1996). Hydrophobic, but not hydrophilic, membranes promote appressoria formation *in vitro* (Lee and Dean, 1994) and hence surface hydrophobicity has been implicated as an important trigger for this process (Talbot *et al*, 1993, 1996; Beckerman and Ebbole, 1996). However, it is unclear whether hydrophobicity is the only signal necessary for appressorium differentiation or whether other surface characteristics are also important.

Several studies have implicated cyclic AMP as a critical mediator of appressorium development in *Magnaporthe* (Mitchell and Dean, 1995; Choi and Dean, 1997). Loss of

*Corresponding author. Fungal Patho-Biology Group, Temasek Life Sciences Laboratory, 1 Research Link, National University of Singapore, Singapore 117604, Singapore. Tel.: +65 6872 7493; Fax: +65 6872 7007; E-mail: naweed@tll.org.sg

Received: 27 June 2006; accepted: 11 December 2006; published online: 25 January 2007

adenylyl cyclase Mac1 or cAMP-dependent protein kinase A activity leads to a failure in appressorium development (Mitchell and Dean, 1995; Choi and Dean, 1997). A MAP kinase cascade has also been identified as an essential signaling pathway involved in appressorium formation during pathogenic growth (Xu and Hamer, 1996; Xu, 2000; Bruno *et al*, 2004).

M. grisea contains three distinct Gα subunits (MagA, MagB and MagC; Liu and Dean, 1997), two Gβ (Mgb1 and Mgb2; Nishimura *et al*, 2003) and one Gγ subunit (MG10193.4; Dean *et al*, 2005). Our sequence comparisons revealed that MagA, MagB and MagC belong to the $G\alpha_s$, $G\alpha_i$ and fungal-specific $G\alpha_{II}$ subfamilies, respectively. Previous characterization of Gα-deletion strains (Liu and Dean, 1997), the *magB*^{G42R} mutant (Fang and Dean, 2000) and the *mgb1*Δ mutant (Nishimura *et al*, 2003) has indicated functions for G-protein signaling in vegetative growth, sexual reproduction and pathogenicity in *M. grisea*. The *mgb1*Δ mutant fails to produce appressoria, whereas elevated Mgb1p levels promote precocious appressoria formation (Nishimura *et al*, 2003).

Here, we describe TMT1398, a novel *Magnaporthe* mutant that uncouples thigmo-morphogenesis (response to mechanical sensation) from hydrophobicity signaling and pathogenesis, and leads to appressoria formation on non-inductive surfaces. TMT1398 harbors a loss-of-function allele of a gene we designate as *RGS1*, as it encodes an RGS domain-containing protein. Based on the characterization of an *rgs1*Δ mutant, we report that surface hardness-dependent signaling is critical for appressorium development. Genetics and biochemical analyses support the notion that Rgs1 is a cross-subfamily regulator of all Gα subunits (MagA, MagB and MagC) and modulates conidiogenesis, surface signaling and pathogenesis in *Magnaporthe*.

Results

Rgs1 is important for proper appressorium differentiation

An insertion mutant, TMT1398, with pleiotropic defects in vegetative growth and appressorium development, was isolated in an *Agrobacterium* Transferred-DNA (T-DNA)-mediated forward screen for nonpathogenic mutants in *M. grisea*. Wild-type conidia could form appressoria only on inductive surface, whereas TMT1398 elaborated appressoria efficiently on the inductive as well as the non-inductive surfaces (Figure 1A). TMT1398 strain was found to contain a single-copy T-DNA insertion that disrupted a candidate gene with extensive sequence similarity to *FLBA* (Yu *et al*, 1996) and *SST2* (Dohlman *et al*, 1996), both of which encode RGS-domain-containing proteins; hence, we designated the TMT1398 locus as *RGS1* in *M. grisea*. Figure 1B schematically shows the T-DNA disruption of the *RGS1* locus in TMT1398 and depicts the *RGS1* annotation on contig 2.276 and 2.277. The full-length cDNA of *RGS1* contains an open reading frame (ORF) encoding a 714-amino acid protein (GenBank accession number DQ335135). The SMART database (http://smart.embl-heidelberg.de) predicts two DEP (Disheveled, Egl-10 and Pleckstrin) domains at the N-terminus and an RGS domain at the C-terminus of the Rgs1 protein (Figure 1B). The primary sequence and predicted secondary structure of the RGS domain from Rgs1 compares favorably to canonical RGS domains using multiple sequence alignment tools (Supplementary Figure S1) suggesting that Rgs1 most likely is a functional GAP.

To ascertain that the defects in TMT1398 were a consequence of the loss of *RGS1* function, we created an *rgs1*Δ strain by replacing the entire ORF of *RGS1* with the hygromycin resistance cassette (*HPH1*; Figure 1B and C). The resultant *rgs1*Δ strain recapitulated the defects shown by TMT1398 and was able to form appressoria on non-inductive membrane surfaces (Figure 1A). Furthermore, genetic complementation using a 7.1-kb fragment carrying the entire *RGS1* locus completely suppressed the appressorial defects of *rgs1*Δ (Figure 1A, complement) and TMT1398 (data not shown). The complemented *rgs1*Δ strain behaved like the wild type, elaborating appressoria only on inductive, but not non-inductive, surfaces (Figure 1A). Based on comparative immunoblotting of Rgs1p levels (Figure 1D and E), the TMT1398 was considered a loss-of-function allele of *RGS1*, as Rgs1 protein was undetectable in the TMT1398 and *rgs1*Δ mutant, but was clearly detected in the wild-type and the complemented strain (Figure 1D). We conclude that the remarkable ability of the TMT1398 and *rgs1*Δ strains to form appressoria on non-inductive surfaces was solely due to the loss of *RGS1*, thus implicating Rgs1 as an important negative regulator of appressorium development and likely an inhibitor of precocious appressorium formation on undesirable surfaces.

Surface hardness stimulus is essential for appressorium differentiation in Magnaporthe

Surface hydrophobicity is considered to be an inductive stimulus for appressorium formation in *Magnaporthe* (Lee and Dean, 1994; Talbot *et al*, 1996). To identify additional signals involved in the regulation of appressorium differentiation, we tested *rgs1*Δ and wild-type strains on artificial surfaces with different physicochemical properties. Neither wax nor petroleum jelly (considered hydrophobic and soft), nor freshly polymerized agar blocks (deemed hydrophilic and soft) could trigger appressorium differentiation in the *rgs1*Δ or wild-type strains (Figure 2A). Germ tube emergence and growth remained unperturbed on both these surfaces. Wild-type *M. grisea* behaved similarly on the non-inductive hydrophilic surface and the soft hydrophobic surface and failed to produce appressoria (Figure 2A), suggesting that surface hydrophobicity alone is not sufficient to induce appressorial development. We concluded that the signaling for appressorium differentiation was not active equivalently on all the surfaces in the *rgs1*Δ strain.

Compared with membrane surfaces used earlier, both petroleum jelly and fresh agar surfaces are softer. We therefore hypothesized that contact with a hard surface might be required for appressorium differentiation. Additional appressorial assays were thus performed on agar surfaces hardened by drying (Figure 2B). Controlled evaporation of water from the agar block did not alter the hydrophilic nature of the surface, as judged by measuring the contact angles made by water droplets on the fresh agar and dried agar surfaces (data not shown; see Supplementary Figure S2). In addition, nano-indentation analyses (Supplementary Figure S2 for methodology) revealed that increasing the drying time increased the hardness of the resultant agar surfaces. Rather strikingly, the ability to induce appressorium development was directly related to surface hardness (Figure 2B). As shown in

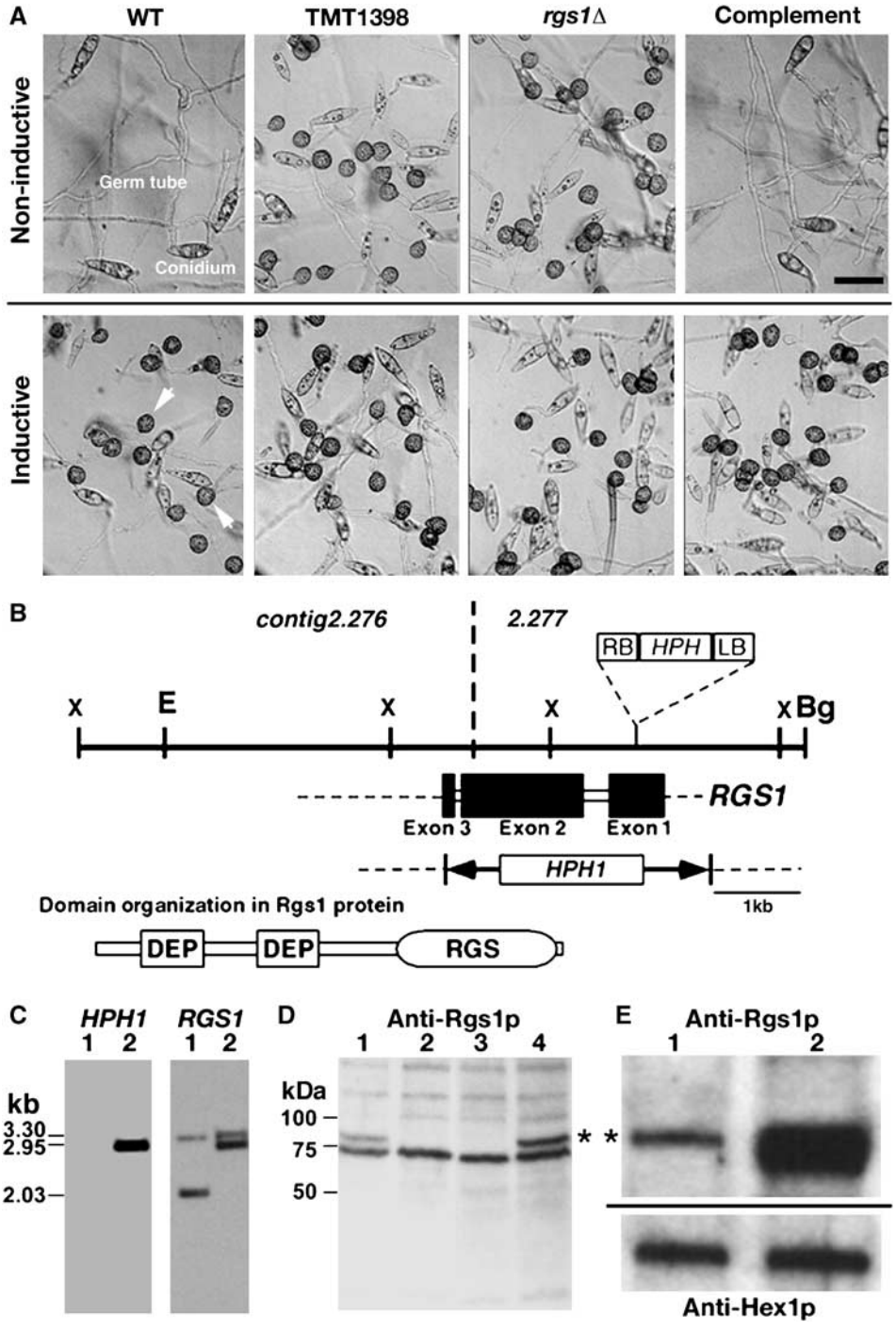

Figure 1 Rgs1 uncouples surface dependency from pathogenic development in *Magnaporthe*. (**A**) Appressorium formation assays on inductive and non-inductive surfaces. Equivalent number of conidia from the wild-type, TMT1398, *rgs1*Δ or the complemented *rgs1*Δ strain were spotted onto indicated surfaces and assessed microscopically for appressoria formation after 16 h. Scale bar represents 20 μm. The fungal structures in question, namely conidium, germ tube and appressorium (arrowheads), are appropriately indicated. (**B**) Schematic representation of the *RGS1* locus in TMT1398 and wild-type strain. RB and LB represent the right and left border sequences, respectively, of the T-DNA integrated in TMT1398, whereas *HPH1* depicts the hygromycin resistance cassette. Solid bars and open boxes depict exons and the introns, respectively, in the *RGS1* locus on the minus strand. Opposing arrows delineate the gene replacement cassette used to create the *rgs1*Δ. DEP and RGS indicate the predicted Pfam domains in the Rgs1 protein. Restriction enzyme sites: X: *Xho*I, E: *Eco*RI and Bg: *Bgl*II. The schematic is drawn to scale (1 kb denoted). (**C**) Southern blot analysis of genomic DNA from the wild type (lane 1) and *rgs1*Δ (lane 2), using *HPH1*-or *RGS1*-specific probes. The estimated sizes of the relevant *Xho*I fragments in kilobase-pair are indicated. (**D**) Both TMT1398 and *rgs1*Δ strain lack Rgs1 protein. Western blot analysis of lysates prepared from the wild-type (1), TMT1398 (2), *rgs1*Δ (3) and the complemented strain (4), using Rgs1 antiserum. Asterisk indicates the Rgs1 protein (M_r 78 kDa). (**E**) Rgs1 overexpression. Total protein lysates from the wild-type (1) and an *RGS1* overexpression strain (2) were immunoblotted with affinity-purified anti-Rgs1p. Subsequently, the blot was reprobed with anti-Hex1p (M_r 18 kDa; Soundararajan *et al*, 2004) as loading control.

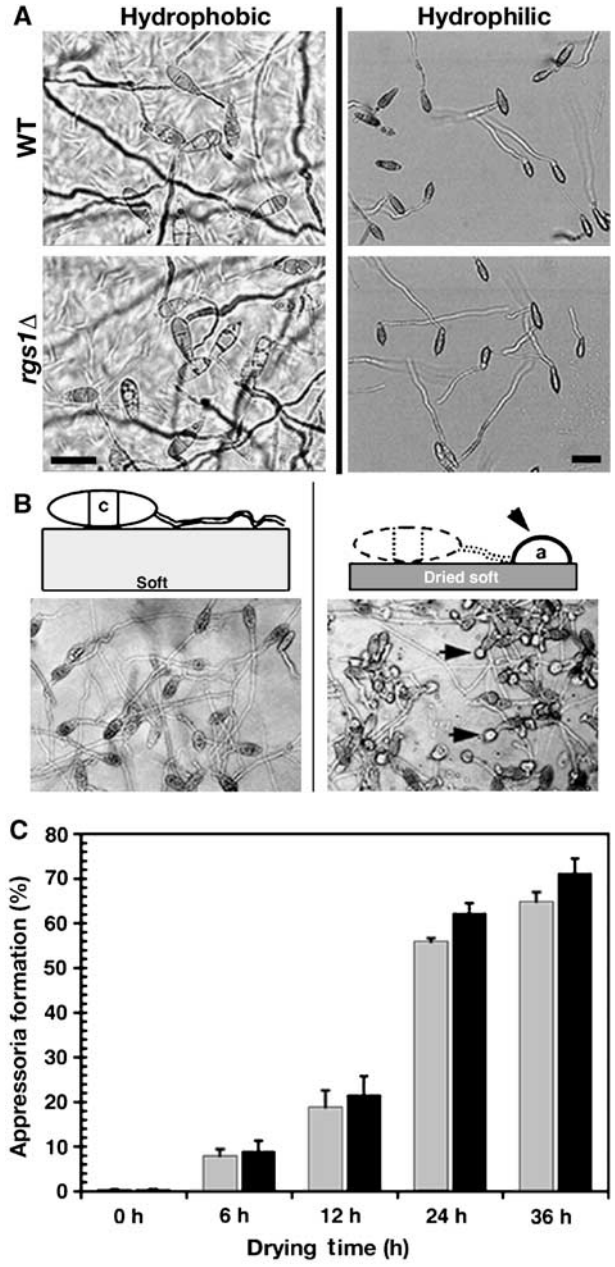

Figure 2 Hardness stimulus is required for appressorium formation in *Magnaporthe*. (**A**) Soft surfaces fail to induce appressoria formation. Conidia from the wild-type or the *rgs1*Δ strain were assessed for appressorium formation on petroleum jelly (hydrophobic) or fresh agar block (hydrophilic). Scale bar represents 20 μm. (**B**) Hard surface induces appressorium development in *Magnaporthe*. Appressorium formation assays using conidial suspension from the *rgs1*Δ (or the WT; quantified in panel C) were performed on 5% fresh agar (soft) or 5% agar blocks dried at 45°C for 24 h (dried soft). Arrows indicate the resultant appressoria on the dried agar surface. (**C**) Increased induction of appressorium formation on hard surface. Equivalent 5% fresh agar blocks were dried for indicated time intervals to attain different hardness levels and seeded with equivalent number of conidia from wild type (gray bars) or *rgs1*Δ (black bars). Resulting appressoria (if any) were quantified after 16 h. Values represent mean ± s.d. from three independent experiments involving 3000 conidia.

Figure 2C, appressoria were rarely elaborated by the wild-type or *rgs1*Δ conidia germinated on fresh agar block, whereas the agar blocks dried for 12 and 24 h could induce appressorium differentiation in 21 ± 3.6 and 62 ± 2.2%, respectively, of the *rgs1*Δ conidia. Under these conditions, appressoria were induced in 18.2 ± 4.3 and 55.7 ± 1.1%, respectively, of the wild-type conidia (Figure 2C). Nano-indentation experiments revealed that the average hardness (mean ± s.d.; 90 indents over three replicates) of the fresh agar block was 73 ± 4 kPa, whereas after drying for 24 h, the resultant hardness of the dried agar block averaged 151 ± 11 kPa. The mean hardness value of a 2-week-old barley leaf was found to be 194 ± 21 kPa. Thus, *RGS1* likely uncouples hardness signal sensing for appressorium development from other inductive stimuli, and that the *rgs1*Δ mutant bypasses the requirement of surface hydrophobicity but not that of surface hardness during appressorium differentiation. Taken together, we conclude that a thigmotropic cue acts as an important trigger for infection-related morphogenesis in *Magnaporthe*.

Timing of the thigmotropic signal sensing

Magnaporthe conidia begin to germinate immediately upon hydration and elaborate short germ tubes within 1–3 h. At about 6 h post inoculation, the tip of the germ tube undergoes swelling and hooks back to initiate appressorium differentiation. To better understand the relationship between surface hardness sensing and appressorium development, we studied the timing of hardness perception. An initial contact for 2 h with a hard surface (GelBond membrane) was sufficient to induce appressorium formation in the *rgs1*Δ (Figure 3B) and the wild-type strain (data not shown). In contrast, a hanging-drop setup that prevented *rgs1*Δ conidia from contacting the hard surface led to a total failure in appressorium formation (Figure 3C). We conclude that contact with a hard surface is necessary for efficient appressorium differentiation, and further suggest that such thigmo-morphogenetic signal is sensed within 2 h of conidial germination.

Rgs1 regulates MagA, the Gα$_s$ subunit, during surface signaling

RGS proteins serve as negative regulators of G-protein signaling by virtue of their ability to accelerate the intrinsic GTPase activity of target Gα subunits. It is thus probable that Rgs1 also functions as a GAP for Gα subunit(s) in *M. grisea*. Therefore, we created individual Gα-deletion mutants (*magA*Δ, *magB*Δ and *magC*Δ) in *Magnaporthe* and analyzed them for defects in appressorium differentiation. A G302S mutation that renders the Gα subunit RGS-insensitive has been characterized in yeast (DiBello *et al*, 1998) and also in mammalian Gα$_o$, Gα$_i$ and Gα$_q$ (DiBello *et al*, 1998; Lan *et al*, 1998). We introduced the corresponding RGS-insensitive mutation (Figure 4A) individually in the three Gα subunits, resulting in *magA*^{G187S}, *magB*^{G183S} and *magC*^{G184S} strains. Like the wild-type, the *magA*Δ strain formed appressoria only on inductive surface (Figure 4B), whereas the *magA*^{G187S} mutant elaborated appressoria efficiently on both the inductive and the non-inductive surfaces, a phenotype reminiscent of *rgs1*Δ.

Next, we created and tested a *magA*^{Q208L} mutant for appressoria formation. The *magA*^{Q208L} corresponds to the Q204L mutation that abolishes the GTPase activity and RGS interaction of the Gα$_s$ subunit (Graziano and Gilman, 1989; Berman *et al*, 1996a) and leads to the constitutive activation of Gα$_s$ owing to higher GTP occupancy. The *magA*^{Q208L} mutant was highly active and elaborated precocious

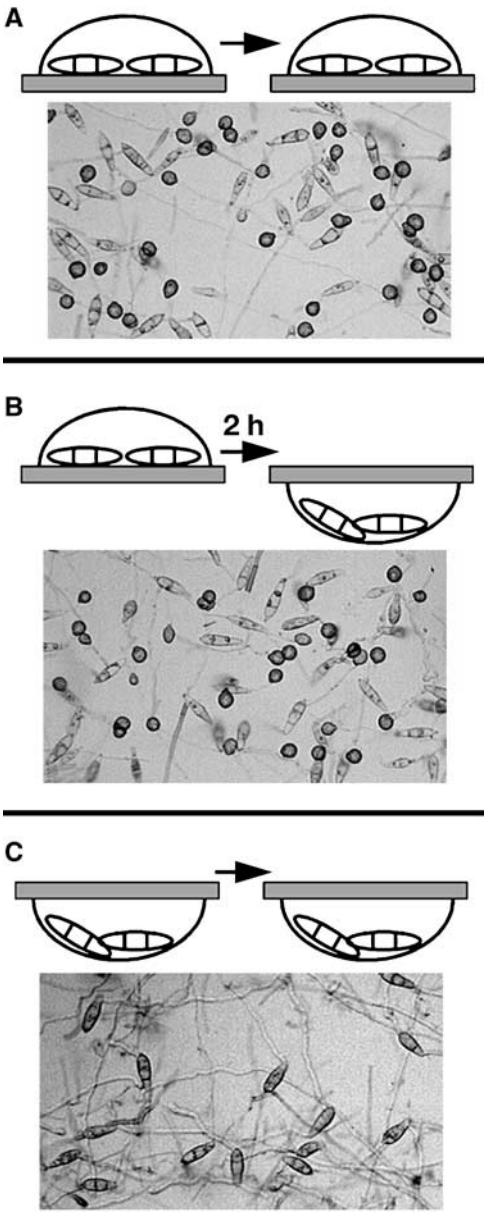

Figure 3 Surface hardness signal is perceived and integrated within 2 h of conidia germination. Appressorium formation was examined under three different conditions of contact between *rgs1*Δ conidia and a hard surface (Gelbond membrane): (**A**) constant contact between conidia and hard surface; (**B**) immediately disengaging the conidia from the hard surface after an initial 2-h contact; (**C**) preventing the conidia–hard surface contact from the start. Images were taken 16 h post inoculation. There was no discernible difference between the *rgs1*Δ and wild-type strains under these conditions (data not shown).

appressoria on inductive and non-inductive surfaces alike (Figure 4B). Compared with the $magA^{G187S}$ mutant, the $magA^{Q208L}$ showed two major differences on the inductive surface: the germ tubes were extremely short and were barely visible in these $magA^{Q208L}$ assays, and secondly, a significant proportion of conidia ($23.7 \pm 2.2\%$; $P = 0.005$) elaborated multiple appressoria from their terminal cells (Figure 4B, inset). These results indicate that Rgs1 genetically interacts with MagA during appressorium development in *Magnaporthe*.

As RGS proteins act by directly binding to their partner Gα subunits (Siderovski and Willard, 2005), we tested whether Rgs1 interacts physically with MagA, by using *Escherichia coli*-purified GST-RGS and MBP-MagA fusion proteins. As shown in Figure 4C, GST-RGS and MBP-MagA proteins indeed interacted in the presence of GDP and AlF_4^-, suggesting that the transition state for nucleotide hydrolysis (Berman *et al*, 1996b) in MagA likely mediates its binding to Rgs1. MBP-MagA could also physically associate with native Rgs1 from the wild-type *M. grisea* strain (Figure 4D). We conclude that Rgs1 physically interacts with, and regulates, MagA during appressorium initiation in *M. grisea*. Additionally, we construe that the GTP-bound MagA serves as a dominant signaling moiety (likely independent of Gβγ) during surface signaling and pathogenic differentiation in *M. grisea*.

As the *magB*Δ strain failed to conidiate, it was impossible to perform appressorium formation assays with this strain. However, examination of the $magB^{G183S}$ (RGS-insensitive) strain indicated that MagB also plays an important role in appressoria formation. On inductive surfaces, the frequency of appressorium formation was similar (~88%) in the $magB^{G183S}$ and wild-type strains. However, on non-inductive surface, the $magB^{G183S}$ showed highly elongated germ tubes and a significant increase in appressoria formation (64 versus 12%) when compared with the wild-type (Supplementary Figure S3). To further confirm these findings and to identify the active state of *magB* during early surface signaling, we tested a GTPase-deficient $magB^{Q204L}$ mutant on the above-mentioned surfaces. Compared with the $magB^{G183S}$, appressoria formation in the $magB^{Q204L}$ mutant was delayed and occurred at a significantly reduced frequency on the inductive as well as the non-inductive surfaces, resulting in highly elongated germ tubes and immature appressoria on both types of surfaces (Supplementary Figure S3). Additionally, we created and analyzed a $magB^{G42R}$ mutant (predicted to be constitutively active) that has been shown to form appressoria on non-inductive surfaces (Fang and Dean, 2000). We found that appressoria formation in the $magB^{G42R}$ mutant was similar to that seen in the $magB^{G183S}$, with germ tubes showing extended growth predominantly on non-inductive surfaces before developing precocious appressoria. Taken together, these data suggest that the $G\alpha_i$ subunit MagB regulates germ tube elongation during the pathogenic phase and, likely through its GTP-bound state, restricts appressorium formation on undesirable surfaces. No defects in appressorium development were evident in *magC*Δ or $magC^{G184S}$ mutants (data not shown).

Rgs1-dependent regulation of cyclic AMP levels

The wild-type strain could not form appressoria on non-inductive surfaces, but addition of the cell-permeable cAMP analog 8-Br-cAMP or the phosphodiesterase inhibitor IBMX to the germinating conidia induced appressorium formation (Figure 5A). These findings were reminiscent of the phenotype of the *rgs1*Δ and $magA^{G187S}$ mutants on non-inductive surfaces. $G\alpha_s$ subunits (such as MagA) function to elevate cAMP levels by directly activating adenylyl cyclase (Tesmer *et al*, 1997b). Therefore, we quantified steady-state cAMP levels in the *rgs1*Δ, $magA^{G187S}$, $magA^{Q208L}$ and wild-type strains. Compared with the wild-type, the levels of cAMP were 4–5-fold higher in the *rgs1*Δ, $magA^{G187S}$ and $magA^{Q208L}$ mutants (Figure 5B). The cAMP levels in the $magB^{Q204L}$

mutant were found to be about 10–15% lower than that in the wild type (data not shown). These observations suggest that $G\alpha_s$ (MagA)-based signaling directly regulates cAMP levels in *Magnaporthe*, and that its activation, owing to the loss/reduction of Rgs1-based negative regulation, likely results in elevated intracellular cAMP levels during the initiation step of pathogenic development.

Relationship between thigmotropism and cAMP levels

Next, we tested whether increasing cAMP levels during conidial germination could help bypass the surface dependency for appressoria formation. Exogenous addition of 8-Br-cAMP was unable to induce appressoria in wild-type conidia inoculated on non-inductive soft surfaces such as agar blocks (Figure 6A). Furthermore, cAMP concentrations as high as 30 mM failed to induce proper appressorium formation in the wild-type conidia seeded on soft agar surfaces. Conidia from wild-type and *rgs1*Δ strains germinated normally on agar blocks containing 10 mM 8-Br-cAMP, but the resultant germ tubes failed to establish the hooking stage necessary to initiate appressoria formation (Figure 6A). Wild-type and *rgs1*Δ conidia germinated efficiently in the presence of 30 mM exogenous 8-Br-cAMP, but the germ tubes showed highly melanized and irregular structures at their tips (Figure 6A). The aberrant apical structures were separated by septa from the germ tube proper (data not shown), but failed to develop into normal appressoria (Figure 6A). Compared with the wild-type, the *rgs1*Δ strain showed an overall higher frequency (2–3-fold) of such aberrant structures upon addition of the equivalent amount of 8-Br-cAMP (30 mM; Figure 6A).

To investigate the relationship between surface hardness stimulus and cAMP, we quantified and compared the intrinsic cAMP levels within the germ tubes produced on hard membrane surfaces to those formed on soft agar surfaces. Steady-state cAMP levels were significantly higher in the germ tubes harvested from the hard hydrophilic surfaces (Figure 6B), suggesting that cAMP accumulation is indeed coupled with proper perception and integration of the initial thigmotropic cue. We thus conclude that during pathogenic development, contact of the germ tubes with a hard surface directly regulates cAMP accumulation, likely through activation of G-protein signaling, and leads finally to formation of functional appressoria.

Rgs1 regulates MagB, the $G\alpha_i$ subunit, during conidiogenesis

Besides its role in appressorium development, Rgs1 was also found to be involved in asexual development (or 'conidiation'). Microscopic observations indicated that *rgs1*Δ colonies produced more conidia than the wild type, and that excess Rgs1 (*RGS1* overexpression) inhibited conidiation

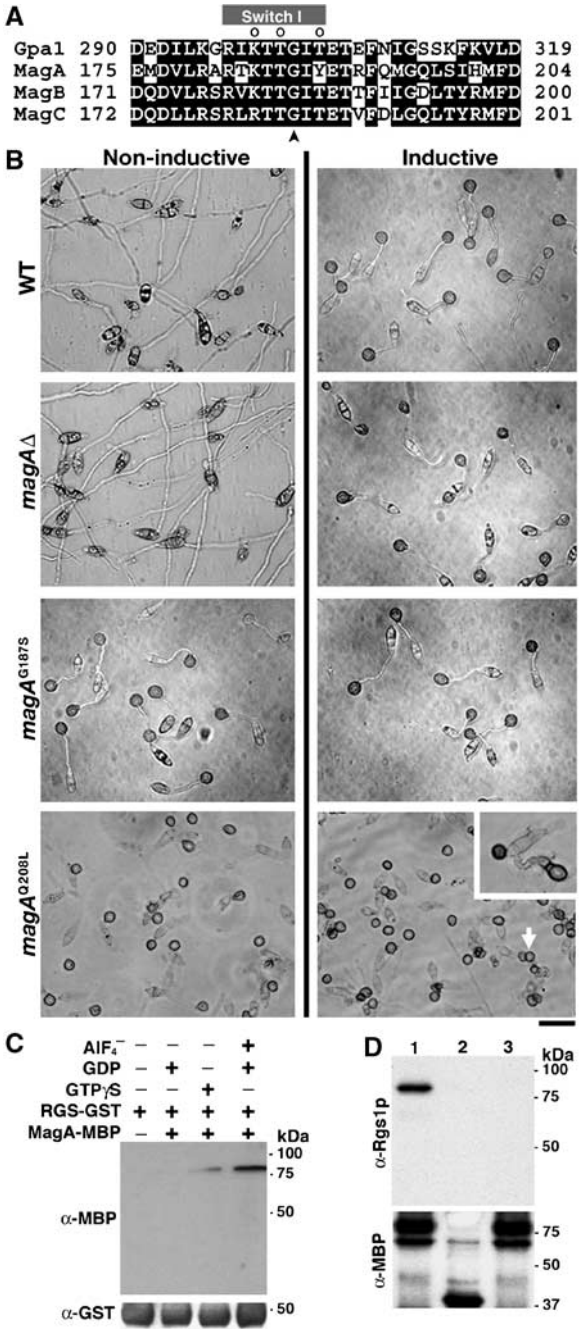

Figure 4 Rgs1 interacts with and regulates MagA for appressorium development. (**A**) Amino-acid sequence alignment of the switch region I of the three Gα subunits in *Magnaporthe* in comparison with the orthologous region from yeast Gpa1. Arrowhead indicates the conserved glycine residue and represents G302 in Gpa1, G187 in MagA, G183 in MagB and G184 in MagC. (**B**) MagA function is required during appressorium development. Appressorium formation assays were performed on non-inductive or inductive surfaces with conidia from the wild-type, $magA^{G187S}$, *magA*Δ and $magA^{Q208L}$ strains. Scale bar denotes 20 μm. Inset depicts a representative image of the aberrant appressoria formation in the $magA^{Q208L}$ strain. (**C**) The RGS domain interacts physically with MagA *in vitro*. *E. coli*-expressed GST-RGS was immobilized on glutathione–Sepharose beads and incubated with purified MBP-MagA in the binding buffer supplemented with GDP, GTPγS or GDP + AlF_4^-. The presence (+) or absence (−) of the indicated component(s) during the binding is listed accordingly. Eluted protein was detected by immunoblotting with monoclonal antibodies against MBP or GST, as indicated. (**D**) Native full-length Rgs1 binds to MBP-MagA. Amylose beads bound to MBP or to purified MBP-MagA fusion protein were incubated with total lysates from wild type or *rgs1*Δ, in the presence of GDP and AlF_4^- (lane 1, MBP-MagA + wild-type lysate; lane 2, MBP + wild-type lysate; lane 3, MBP-MagA + *rgs1*Δ lysate). The bead-associated proteins were fractionated by SDS–PAGE and analyzed by Western blotting with Rgs1 antiserum and subsequently reprobed with MBP antisera.

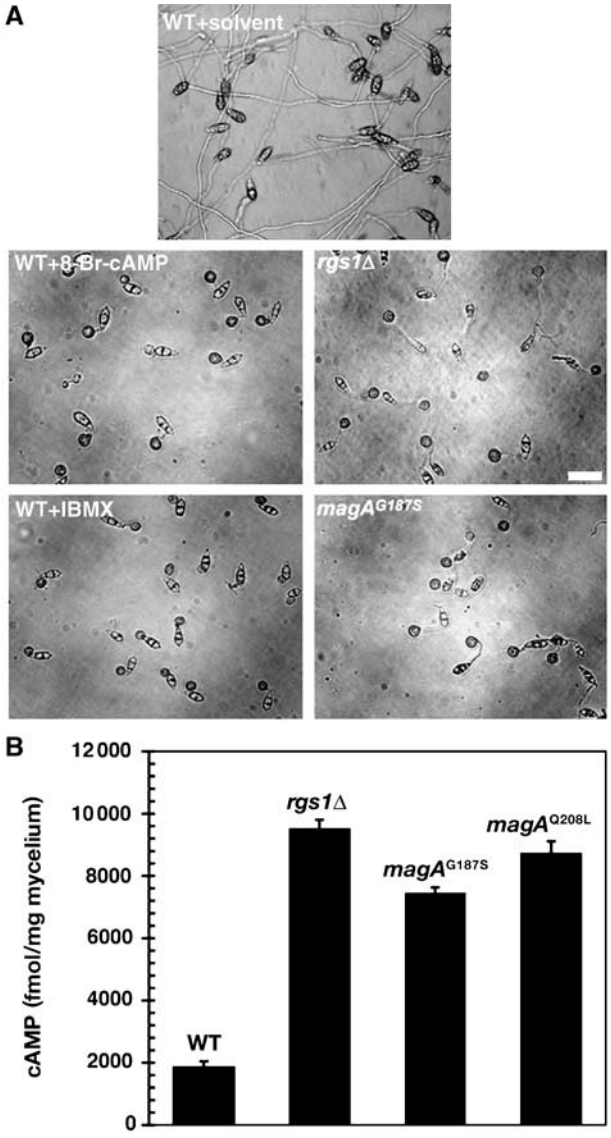

Figure 5 Rgs1 and MagA regulate intracellular cAMP levels during pathogenesis. (**A**) 8-Br-cAMP or IBMX induces appressorium formation on non-inductive hard surfaces. Wild-type conidia were assessed for appressoria formation in the absence (WT + solvent) or presence of 8-Br-cAMP or IBMX. Appressorium formation in the *rgs1*Δ or *magA*^{G187S} served as controls in parallel. Scale bar denotes 20 μm. (**B**) Loss of Rgs1 leads to increased accumulation of cAMP. Bar chart showing quantification of intracellular cAMP in the mycelia of the indicated strains cultured for 2 days in complete medium in the presence of IBMX. Values represent mean ± s.d. from two independent experiments with three replicates each.

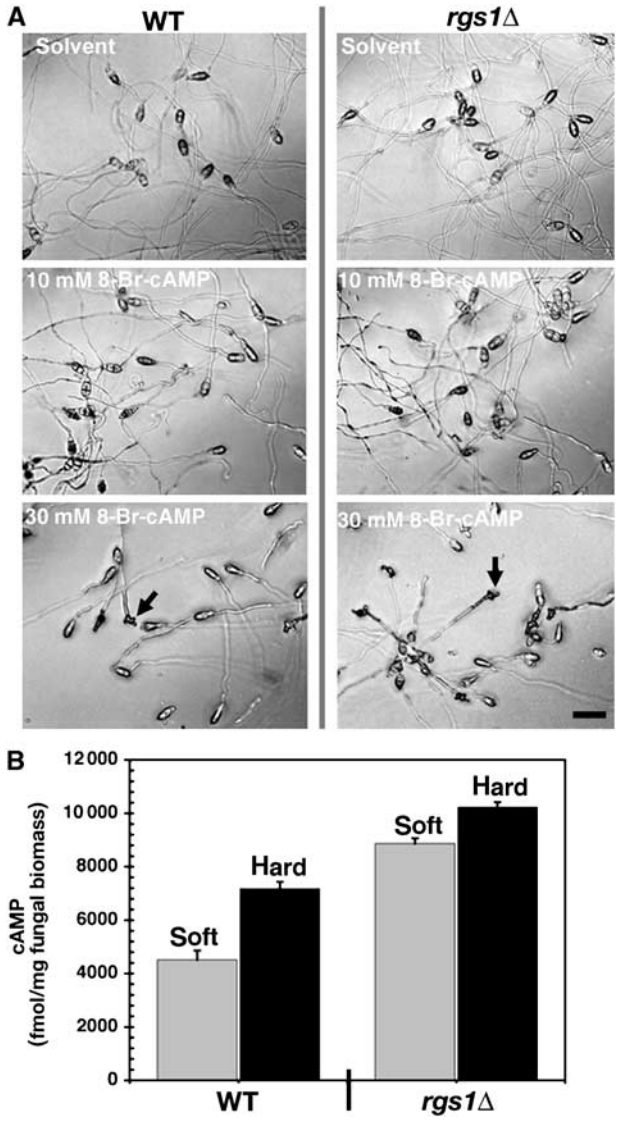

Figure 6 Sensing of surface hardness and regulation of intracellular cAMP. (**A**) Exogenous addition of 8-Br-cAMP fails to induce appressorium development on soft surfaces. Conidia from the wild type (WT) or the *rgs1*Δ were assessed for appressorium formation on fresh agar blocks in the presence of the indicated amounts of 8-Br-cAMP. Arrows indicate aberrant and irregular melanized structures formed. (**B**) Effect of surface hardness signaling on cAMP levels. Equivalent number of conidia from the WT or the *rgs1*Δ strain was germinated on soft (1% agar) or hard (GelBond membrane) surfaces for 3 h, and the internal cAMP levels were quantified immediately. Values represent mean (± s.d.) from two independent experiments with three replicates each.

(Figure 7A). This implicated Rgs1 as a negative regulator of conidiation in *Magnaporthe*. We examined conidiation in Gα-deletion mutants (*magA*Δ, *magB*Δ and *magC*Δ), RGS-insensitive mutants (*magA*^{G187S}, *magB*^{G183S} and *magC*^{G184S}) and GTPase-deficient alleles of *magA* and *magB*. Loss of *MAGB* function completely abolished conidiation, whereas the *magB*^{G183S}, *magB*^{Q204L} and *magB*^{G42R} mutants each showed hyper-conidiation defects (Figure 7A). Furthermore, the increased ability to conidiate in the *rgs1*Δ strain was completely abolished upon deletion of the *MAGB* gene, and the resultant *rgs1*Δ *magB*Δ double mutant did not conidiate at all (Figure 7A). No apparent conidiation defects were evident in the *magA*Δ, *magA*^{G187S}, *magC*Δ or *magC*^{G184S} mutants. A surprising finding was the significant reduction (~87%) in conidiation in the *magA*^{Q208L} mutant. This decrease in conidiation was most likely a consequence of the huge reduction in the number of aerial hyphae and conidiophores in the *magA*^{Q208L} mutant (Figure 7A). The *magA*^{Q208L} strain also showed precocious pigmentation at the tips of the aerial hyphae and the conidiophores (Figure 7A). The bar chart in Figure 7B depicts the quantification of the total number of conidia produced by the respective mutants mentioned above. We conclude that Rgs1 and MagB act in concert to regulate conidia formation in *Magnaporthe* and infer that the

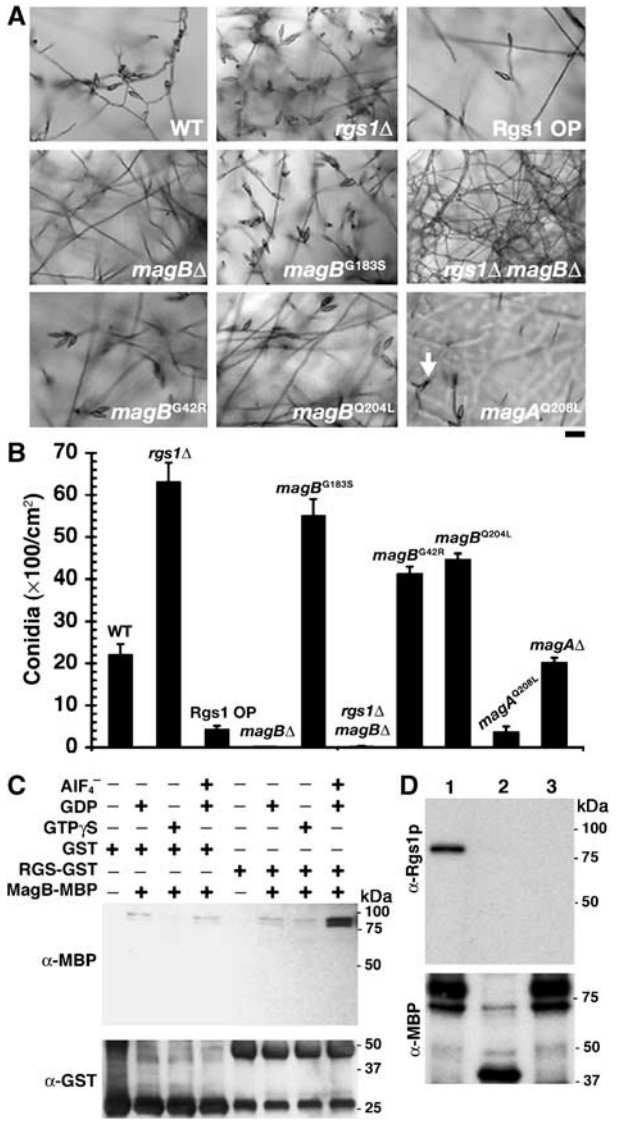

Figure 7 Rgs1 physically interacts with and regulates MagB during asexual development. (**A**) Evaluation and quantification of conidiogenesis. Strains of the indicated genotypes were cultured in dark for 3 days at 28°C and then grown further for 6 days under constant illumination. Aerial hyphae on the surface of the colonies were imaged. Arrowhead indicates precocious melanization of conidiophores in the *magA*^{Q208L} strain. (**B**) Conidiation defects in *rgs1*Δ and *magB*Δ strains. Conidia produced by the indicated strains were harvested and quantified. Data represent the mean values (±s.d.) from three independent experiments. (**C**) The RGS domain interacts with Gα$_i$ subunit MagB *in vitro*. Purified GST-RGS and MBP-MagB proteins were used to perform protein binding assay as described in Figure 4C. The protein complex was fractionated by SDS–PAGE and analyzed by Western blotting using antisera against MBP or GST. (**D**) Native full-length Rgs1 binds MBP-MagB. Total lysates from the wild-type (lane 1) or *rgs1*Δ (lane 3) strain were used in a pull-down assay with MBP-MagB, as described earlier in Figure 4D. MBP interaction with the wild-type lysate (lane 2) was used as control. Bead-associated proteins were purified and subjected to Western blotting with Rgs1 antiserum or anti-MBP.

GTP-bound MagA likely functions as a negative regulator of aerial hyphae and conidiophore development.

E. coli-purified GST-RGS and MBP-MagB fusion proteins were found to physically interact in a GDP·AlF_4^--dependent manner (Figure 7C). Moreover, full-length Rgs1 protein was found to associate with MBP-MagB in pull-down assays using total lysates from wild-type but not from *rgs1*Δ (Figure 7D). We conclude that Rgs1 physiologically interacts with, and regulates, the Gα$_i$ MagB during conidiation in *M. grisea*.

Discussion

Physicochemical properties of the plant surface, which can be mimicked *in vitro* to some extent, are believed to trigger the formation of appressoria in *M. grisea*. Surface hydrophobicity is considered to be important, as wild-type conidia form appressoria on hydrophobic, but not hydrophilic, surfaces, thus leading to a general classification of these two surfaces as inductive and non-inductive, respectively. In this study, we characterized a novel *Magnaporthe* mutant, TMT1398, which abolished surface dependency during appressoria formation and responded efficiently to inductive, as well as non-inductive, surfaces. Through genetic complementation analysis, we ascertained that the defects in TMT1398 (and an *rgs1*Δ mutant) were due solely to the loss of Rgs1 protein, thus implicating Rgs1 to be a negative regulator of appressoria formation that couples surface dependency with infection-related morphogenesis.

A rather surprising finding was the inability of wild type and *rgs1*Δ to elaborate appressoria on softer surfaces irrespective of their hydrophobic or hydrophilic nature. This suggested that surface hydrophobicity alone is insufficient to induce appressorium development, and that soft surfaces such as agar blocks or wax are non-inductive. Surface hardness, thus, represents a critical signal for appressorium development, as observed in appressorium formation assays on dried agar surfaces (derived from non-inductive fresh agar blocks), where *rgs1*Δ and wild-type were now fully capable of forming functional appressoria. We estimated the critical surface hardness required for initiating appressoria, and also demonstrated that the accumulation of cAMP, an important second messenger (Lee and Dean, 1993; Choi and Dean, 1997), depends on contact with a requisite hard surface. Furthermore, exogenous addition of 8-Br-cAMP to germinating wild-type or *rgs1*Δ conidia failed to induce appressoria on soft surfaces. This suggests that although cAMP-mediated signaling is essential, it is not sufficient to initiate appressoria on inappropriate surfaces and that contact with a hard surface is indeed necessary to trigger pathogenic behavior. Initiation of appressoria on leaf surfaces or on hydrophobic hard surfaces was comparatively more efficient than it was on dried agar surfaces, thus implying that surface hardness, as well as hydrophobicity, is important for efficient development of appressoria in *M. grisea*.

As Rgs1 showed a high degree of similarity to G-protein regulators FlbA (Yu *et al*, 1996), Sst2 (Dohlman *et al*, 1996) and CpRGS1 (Segers *et al*, 2004), we investigated the function(s) of Gα subunits MagA, MagB and MagC as potential substrates of Rgs1 GAP activity. Interestingly, the RGS-insensitive Gα$_S$ *magA*^{G187S} and the GTPase-deficient *magA*^{Q208L} were each capable of forming appressoria on both the inductive and non-inductive surfaces similar to the *rgs1*Δ strain. Furthermore, Rgs1 physically interacted with an activated form of MagA, thus suggesting that Rgs1 directly regulates MagA during appressoria initiation. Like the *rgs1*Δ, the *magA*^{G187S} and *magA*^{Q208L} strains accumulated high levels of cAMP, suggesting that a role for Rgs1 in

appressorium formation is to regulate the nucleotide state of MagA and thereby control GTP-MagA-dependent adenylyl cyclase activation and the resultant levels of intracellular cAMP. Comparative analysis of the *magA*^{Q208L} and *magA*^{G183S} mutants showed that GTP-MagA is indeed a dominant signaling moiety that likely activates downstream effector(s) independent of the Gβγ dimer. These data help explain the lack of appressorial defects in the *magA*Δ strain and are consistent with earlier results related to the Gβ subunit in *M. grisea* (Nishimura *et al*, 2003).

Analysis of the *magB*^{G183S}, *magB*^{G42R} and *magB*^{Q204L} strains revealed that a probable function of GTP-bound MagB is to suppress appressoria formation on undesirable surfaces, indirectly resulting in extensive elongation of germ tubes. The duration and strength of G-protein-mediated signaling is regulated by the rate at which GTP is hydrolyzed by Gα (Dohlman and Thorner, 2001). It is probable that GTP hydrolysis is weak or insufficient in the *magB*^{G183S} mutant (and residual in the *magB*^{G42R} mutant), thus delaying the reassociation of the Gβγ dimer with the mutant *magB* alleles. We believe that delayed appressorium formation in the *magB* mutants partly reflects the counteracting function(s) of the dissociated Gβγ and the compromised GTPase function that increases the GTP occupancy variably on these mutant MagB variants. A preliminary finding that cAMP levels are subnormal in the *magB*^{Q204L} mutant supports a possibility that GTP-MagB, true to its Gα_i subfamily classification, inhibits adenylyl cyclase activity in *M. grisea*. In future experiments, we will focus on discerning the exact role of MagB in regulating the accumulation of appressorial cAMP.

FlbA and CpRGS1 are both known to positively regulate asexual development (Yu *et al*, 1996; Segers *et al*, 2004). In contrast, we found that Rgs1 negatively regulates conidiation in *M. grisea*. Elevated Rgs1 levels inhibited conidiation, whereas loss of Rgs1 led to profuse conidiation. An unexpected finding was the inhibitory role of GTP-bound MagA (based on *magA*^{Q208L}) during the differentiation of aerial hyphae and conidiophores, indirectly leading to reduced conidiation. It remains to be seen if such reduction in aerial growth (and conidiation) is due to the excessive cAMP in the *magA*^{Q208L} strain. However, Rgs1 function during conidia formation *per se* was mediated primarily through regulation of MagB. MagB was found to be essential for conidiation, and deletion of *MAGB* in the *rgs1*Δ background abolished the production of conidia. Furthermore, the *magB*^{G183S}, *magB*^{G42R} and *magB*^{Q204L} mutants showed excessive conidiation reminiscent of the *rgs1*Δ strain. These data suggest that GTP-bound MagB is likely a major signaling moiety during conidia formation. The genetic interactions discussed above were ably supported by biochemical studies that showed Rgs1 physically interacts with MagB, in a manner suggesting a possible GAP activity for Rgs1.

Interestingly, we also found direct interactions between activated MagC (Gα_{II} subunit) and Rgs1 in *M. grisea* (Supplementary Figure S5). Although its biological significance is presently unclear, preliminary results implicate MagC in the maintenance of mycelial hydrophobicity during vegetative growth (data not shown). Overall, our findings suggest that Rgs1 is a unique regulator of G-protein signaling and negatively controls three distinct Gα subunits during different, albeit very important, biological functions such as asexual development, vegetative growth and infection-related morphogenesis in the model phytopathogen *M. grisea*.

Future experiments will be aimed at identifying the molecular basis of thigmotropism in *Magnaporthe*, and its functional relevance (if any) to heterotrimeric G-protein signaling. Additionally, we hope to identify the specific downstream effector(s) of the individual Gα subunits during the developmental stages mentioned above. We also intend to analyze whether G proteins serve specific function(s) during the host penetration and *in planta* developmental phase in *Magnaporthe*.

Materials and methods

Fungal strains and culture conditions

The *M. grisea* wild-type strain B157 was obtained from the Directorate of Rice Research (Hyderabad, India). For culture maintenance and conidiation, wild-type and mutant strains were grown on prune agar medium (PA) as described (Soundararajan *et al*, 2004). Mycelia used for genomic DNA, total RNA and total protein extraction were harvested from cultures grown in liquid complete medium (CM) for 2 days.

Appressorium formation assay

Conidia harvested from 10-day-old cultures were filtered through Miracloth (Calbiochem, CA, USA) and resuspended to 1×10^5 conidia per milliliter in sterile water. Droplets (20–50 μl) of conidial suspension were placed on membranes or other tested surfaces and incubated under humid conditions at room temperature. Microscopic observations were made at requisite intervals. Treatment with IBMX (2.5 mM) or 8-Br-cAMP (at 10 or 30 mM) was carried out for 16 h. Photomicrographs were taken using a Nikon Eclipse 80i compound microscope with differential interference contrast optics.

Isolation of TMT1398 and molecular cloning of RGS1

The *M. grisea* mutant TMT1398 was isolated in an *Agrobacterium* T-DNA-mediated insertional mutagenesis screen for pathogenesis-related defects (H Liu and NI Naqvi, unpublished data). Genomic DNA extracted from TMT1398 was digested with restriction enzyme *Bgl*II and used for Southern analysis to determine the number of T-DNA insertion sites. DNA sequences flanking the single T-DNA insertion in TMT1398 were amplified using the TAIL PCR method (Liu and Whittier, 1995) and sequenced. Full-length cDNA encoded by the candidate gene, *RGS1*, disrupted in TMT1398, was obtained with primers NIN749 and NIN670 using a one-step RT–PCR kit (Qiagen Corporation, USA). The *Magnaporthe* Genome Database (http://www.broad.mit.edu/annotation/fungi/magnaporthe; Dean *et al*, 2005) was used to anchor the *RGS1* locus to the genome contig(s) and the requisite overlapping clones obtained from a BAC library (Clemson University Genomics Institute, USA).

RGS1 deletion, complementation analysis and RGS1 overexpression

The *RGS1*-deletion mutant was generated using the standard one-step gene replacement strategy. Briefly, about 1 kb of 5′ UTR and 3′ UTR regions was PCR amplified (see Supplementary Figure S4 for primer sequences and restriction enzyme sites) and ligated sequentially to flank the hygromycin resistance cassette in pFGL59. The gene replacement construct was introduced into *M. grisea* B157 via *Agrobacterium*-mediated transformation. CM containing 250 μg/ml hygromycin was used for selection. Correct gene replacement event (*rgs1*::*HPH1*) was confirmed by PCR and Southern analysis. A 7.1-kb *Bgl*II–*Eco*RI fragment from BAC clone 02N7, which contained the entire *RGS1* locus, was cloned into the *Bam*HI–*Eco*RI sites in pFGL97 (bialaphos resistance) and used to complement the *rgs1*Δ strain. Resistance to ammonium glufosinate (Cluzeau Labo, France) was used to select the requisite transformants, and single-copy integrants ascertained by DNA gel blots.

Gα-deletion mutants and site-directed mutagenesis

The same strategy as used for the *RGS1* deletion was followed to individually delete the Gα genes, using their respective 5′ UTR and 3′ UTR fragments. Two fragments amplified with primers

NIN577/NIN578 and NIN579/NIN580, respectively, were cloned subsequently and used for *MAGA* deletion. The primer pairs NIN714/NIN715 and NIN716/NIIN717 were similarly used to amplify fragments for *MAGB* replacement, and primer pairs NIN573/NIN574 and NIN575/NIN576 for *MAGC* deletion (Supplementary Figure S4).

For creating RGS-insensitive mutations (G302S equivalents) in the Gα subunits, we introduced the desired mutation on the PCR fragments used for making the constructs, which were then used for homology-dependent replacement of the WT locus with the mutant allele, such that in each instance the mutant allele was the sole copy of that particular Gα and was placed under its native regulation. For *MAGA*, the fragment amplified with primers NIN865/866 was cloned into the *Pst*I and *Hin*dIII sites in pFGL347 to obtain pFGL369. Fragments amplified with primers NIN861/NIN862 (*Xho*I/*Spe*I) and NIN863/NIN864 (*Spe*I/*Eco*RI) were cloned into the *Xho*I–*Eco*RI sites of pFGL369 (hygromycin resistance). The resultant pFGL370 was introduced into *M. grisea* B157 to finally obtain the $magA^{G187S}$ mutant strains. A similar strategy was used to create the $magA^{Q208L}$, $magB^{G183S}$, $magB^{G42R}$, $magB^{Q204L}$ and $magC^{G184S}$ strains. The mutant alleles were confirmed by requisite PCR amplification and sequencing analyses. The primers used in each instance are listed in Supplementary Figure S4.

Rgs1 antiserum and protein analysis

A fusion protein containing the GST tag and the proximal 1–531 aa of Rgs1 was expressed in *E. coli* BL21(DE3) and purified using glutathione–Sepharose 4B (Amersham Biosciences, USA) and eluted with 10 mM GSH. A total of 500 μg (1 mg/ml) GST-RGS protein was emulsified with an equal volume of adjuvant and injected intramuscularly into 2-month-old New Zealand White female rabbits. Rabbits were boosted at 2-week intervals. Antiserum specificity was ascertained by Western blot analysis of total protein lysates from wild-type and *rgs1*Δ mycelia. Rgs1 antiserum was affinity purified using standard protocols.

Protein-related methods

Total protein extracts were obtained by grinding 2-day-old mycelial cultures in liquid nitrogen and resuspended in 300 μl of extraction buffer (10 mM Na_2HPO_4 pH 7.0, 0.5% SDS, 1 mM DTT and 1 mM EDTA). Lysates were cleared by centrifugation at 12 000 *g* for 20 min at 4°C. Protein concentrations in the supernatant were determined by the Bradford assay (Bio-Rad, USA). Protein sample (100 μg) from each extract was fractionated by SDS–PAGE, transferred onto a PVDF membrane (Millipore Corporation, USA) and immunoblotted with Rgs1 antiserum (1:1000 dilution). Secondary antibodies conjugated to horseradish peroxidase were used at 1:10 000 dilution. The SuperSignal kit (Pierce, USA) was used to detect the chemiluminescent signals as instructed.

To examine the *in vitro* interaction between RGS domain and Gα proteins, 40 μg of GST or GST-RGS (amino acids 531–714) bound to glutathione-conjugated beads was incubated for 30 min at room temperature in binding buffer (50 mM Tris–HCl, pH 7.5, 50 mM NaCl and 2 mM DTT) supplemented with 50 μM GDP, 50 μM GTPγS and 5 mM $MgCl_2$ or 50 μM GDP, 5 mM $MgCl_2$, 10 mM NaF and 30 μM $AlCl_3$. Then, 80 μg MBP-MagA or MBP-MagB or MBP-MagC protein was added and incubated at 4°C for 2 h. The beads were washed five times with the binding buffer containing the respective nucleotides and/or $AlCl_3$ and NaF. The agarose beads and associated proteins were boiled for 6 min, fractionated on SDS–PAGE and immunoblotted with anti-MBP or anti-GST antisera (Sigma-Aldrich, USA).

To obtain total lysates, mycelia were ground into a fine powder and extracted with non-denaturing NP-40 buffer (6 mM Na_2HPO_4, 4 mM NaH_2PO_4, 1% Triton X-100, 200 mM NaCl and 2 mM EDTA). The crude lysate was mixed with MBP or MBP-MagA or MBP-MagB or MBP-MagC proteins, conjugated to amylose beads for 2 h at 4°C in the presence of 50 μM GDP, 5 mM $MgCl_2$, 10 mM NaF and 30 μM $AlCl_3$. The beads were washed five times with the binding buffer. Affinity-purified proteins were immunoblotted with anti-Rgs1 and later reprobed with anti-MBP.

Quantification of intracellular cAMP

Two-day-old liquid mycelial cultures, or conidia germinated for 3 h on 1% soft agar surface or hydrophilic GelBond membranes (Cambrex BioScience, USA), were harvested, frozen in liquid nitrogen and lyophilized for 16 h. The dried samples were individually ground to a fine powder in liquid nitrogen and resuspended in 200 μl ice-cold 6% TCA and incubated on ice for 10 min. After centrifugation at 4000 r.p.m. for 15 min at 4°C, the supernatant was collected and washed four times with five volumes of water-saturated diethyl ether. The remaining aqueous extract was lyophilized and dissolved in the assay buffer. The cAMP levels were quantified according to the cAMP Biotrak Immuno-assay System (Amersham Biosciences, NJ, USA).

Supplementary data

Supplementary data are available at *The EMBO Journal* Online (http://www.embojournal.org).

Acknowledgements

We thank members of the Fungal Patho-Biology Group for helpful suggestions and discussions. We thank S Naqvi, G Jedd and S Oliferenko for comments on the manuscript. Work in the Siderovski laboratory was funded by NIH grant R01 GM074268. This work was supported by intramural research funds (to NIN) from Temasek Life Sciences Laboratory, Singapore.

References

Beckerman JL, Ebbole DJ (1996) MPG1, a gene encoding a fungal hydrophobin of *Magnaporthe grisea*, is involved in surface recognition. *Mol Plant Microbe Interact* **9:** 450–456

Berman DM, Kozasa T, Gilman AG (1996b) The GTPase-activating protein RGS4 stabilizes the transition state for nucleotide hydrolysis. *J Biol Chem* **271:** 27209–27212

Berman DM, Wilkie TM, Gilman AG (1996a) GAIP and RGS4 are GTPAse-activating proteins for the G_i subfamily of G protein α subunits. *Cell* **86:** 445–452

Bolker M (1998) Sex and crime: heterotrimeric G proteins in fungal mating and pathogenesis. *Fungal Genet Biol* **25:** 143–156

Bruno KS, Tenjo F, Li L, Hamer JE, Xu JR (2004) Cellular localization and role of kinase activity of PMK1 in *Magnaporthe grisea*. *Eukaryot Cell* **3:** 1525–1532

Castellone MD, Teramoto H, Williams BO, Druey KM, Gutkind JS (2005) Prostaglandin E2 promotes colon cancer cell growth through a Gs–axin-beta-catenin signaling axis. *Science* **310:** 1504–1510

Choi W, Dean RA (1997) The adenylate cyclase gene MAC1 of *Magnaporthe grisea* controls appressorium formation and other aspects of growth and development. *Plant Cell* **9:** 1973–1983

Dean RA, Talbot NJ, Ebbole DJ, Farman ML, Mitchell TK, Orbach MJ, Thon M, Kulkarni R, Xu JR, Pan H, Read ND, Lee YH, Carbone I, Brown D, Oh YY, Donofrio N, Jeong JS, Soanes DM, Djonovic S, Kolomiets E, Rehmeyer C, Li W, Harding M, Kim S, Lebrun MH, Bohnert H, Coughlan S, Butler J, Calvo S, Ma LJ, Nicol R, Purcell S, Nusbaum C, Galagan JE, Birren BW (2005) The genome sequence of the rice blast fungus *Magnaporthe grisea*. *Nature* **434:** 980–986

DiBello PR, Garrison TR, Apanovitch DM, Hoffman G, Shuey DJ, Mason K, Cockett MI, Dohlman HG (1998) Selective uncoupling of RGS action by a single point mutation in the G protein alpha-subunit. *J Biol Chem* **273:** 5780–5784

Dohlman HG, Song J, Ma D, Courchesne WE, Thorner J (1996) Sst2, a negative regulator of pheromone signaling in the yeast *Saccharomyces cerevisiae*: expression, localization, and genetic interaction and physical association with Gpa1 (the G-protein alpha subunit). *Mol Cell Biol* **16:** 5194–5209

Dohlman HG, Thorner JW (2001) Regulation of G protein-initiated signal transduction in yeast: paradigms and principles. *Annu Rev Biochem* **70:** 703–754

Fang EG, Dean RA (2000) Site-directed mutagenesis of the *magB* gene affects growth and development in *Magnaporthe grisea*. *Mol Plant Microbe Interact* **13:** 1214–1227

Fukuhara S, Chikumi H, Gutkind JS (2001) RGS-containing RhoGEFs: the missing link between transforming G proteins and Rho? *Oncogene* **20:** 1661–1668

Gilbert RD, Johnson AM, Dean RA (1996) Chemical signals responsible for appressorium formation in the rice blast fungus *Magnaporthe grisea*. *Physiol Mol Plant Pathol* **48:** 335–346

Graziano MP, Gilman AG (1989) Synthesis in *Escherichia coli* of GTPase-deficient mutants of Gs_{α}. *J Biol Chem* **264:** 15475–15482

Koelle MR, Horvitz HR (1996) EGL-10 regulates G protein signaling in the *C. elegans* nervous system and shares a conserved domain with many mammalian proteins. *Cell* **84:** 115–125

Lan KL, Sarvazyan NA, Taussig R, Mackenzie RG, DiBello PR, Dohlman HG, Neubig RR (1998) A point mutation in Galphao and Galphai1 blocks interaction with regulator of G protein signaling proteins. *J Biol Chem* **273:** 12794–12797

Lee YH, Dean RA (1993) cAMP regulates infection structure formation in the plant pathogenic fungus *Magnaporthe grisea*. *Plant Cell* **5:** 693–700

Lee YH, Dean RA (1994) Hydrophobicity of the contact surface induces appressorium formation in *Magnaporthe grisea*. *FEMS Microbiol Lett* **115:** 71–76

Lengeler KB, Davidson RC, D'Souza C, Harashima T, Shen WC, Wang P, Pan X, Waugh M, Heitman J (2000) Signal transduction cascades regulating fungal development and virulence. *Microbiol Mol Biol Rev* **64:** 746–785

Liu S, Dean RA (1997) G protein alpha subunit genes control growth, development, and pathogenicity of *Magnaporthe grisea*. *Mol Plant Microbe Interact* **10:** 1075–1086

Liu YG, Whittier RF (1995) Thermal asymmetric interlaced PCR: automatable amplification and sequencing of insert end fragments from P1 and YAC clones for chromosome walking. *Genomics* **25:** 674–681

Malbon CC (2005) G proteins in development. *Nat Rev Mol Cell Biol* **6:** 689–701

Mitchell TK, Dean RA (1995) The cAMP-dependent protein kinase catalytic subunit is required for appressorium formation and pathogenesis by the rice blast pathogen *Magnaporthe grisea*. *Plant Cell* **7:** 1869–1878

Nishimura M, Park G, Xu JR (2003) The G-beta subunit MGB1 is involved in regulating multiple steps of infection-related morphogenesis in *Magnaporthe grisea*. *Mol Microbiol* **50:** 231–243

Ou SH (1985) *Rice Diseases*, 2nd edn, Surrey, UK: Commonwealth Mycology Institute

Segers GC, Regier JC, Nuss DL (2004) Evidence for a role of the regulator of G-protein signaling protein CPRGS-1 in Galpha subunit CPG-1-mediated regulation of fungal virulence, conidiation, and hydrophobin synthesis in the chestnut blight fungus *Cryphonectria parasitica*. *Eukaryot Cell* **3:** 1454–1463

Siderovski DP, Hessel A, Chung S, Mak TW, Tyers M (1996) A new family of regulators of G-protein-coupled receptors. *Curr Biol* **6:** 211–212

Siderovski DP, Willard FS (2005) The GAPs, GEFs and GDIs of heterotrimeric G-protein alpha subunits. *Int J Biol Sci* **1:** 51–66

Slep KC, Kercher MA, He W, Cowan CW, Wensel TG, Sigler PB (2001) Structural determinants for regulation of phosphodiesterase by a G protein at 2.0 A. *Nature* **409:** 1071–1077

Soundararajan S, Jedd G, Li X, Ramos-Pamplona M, Chua NH, Naqvi NI (2004) Woronin body function in *Magnaporthe grisea* is essential for efficient pathogenesis and for survival during nitrogen starvation stress. *Plant Cell* **16:** 1564–1574

Talbot NJ, Ebbole DJ, Hamer JE (1993) Identification and characterization of MPG1, a gene involved in pathogenicity from the rice blast fungus *Magnaporthe grisea*. *Plant Cell* **5:** 1575–1590

Talbot NJ, Kershaw MJ, Wakley GE, De Vries O, Wessels J, Hamer JE (1996) MPG1 encodes a fungal hydrophobin involved in surface interactions during infection-related development of *Magnaporthe grisea*. *Plant Cell* **8:** 985–999

Tesmer JJ, Berman DM, Gilman AG, Sprang SR (1997a) Structure of RGS4 bound to AlF_4^--activated G(i alpha1): stabilization of the transition state for GTP hydrolysis. *Cell* **89:** 251–261

Tesmer JJ, Sunahara RK, Gilman AG, Sprang SR (1997b) Crystal structure of the catalytic domains of adenylyl cyclase in a complex with Gsalpha.GTPgammaS. *Science* **278:** 1907–1916

Xu JR (2000) MAP kinases in fungal pathogens. *Fungal Genet Biol* **31:** 137–152

Xu JR, Hamer JE (1996) MAP kinase and cAMP signaling regulate infection structure formation and pathogenic growth in the rice blast fungus *Magnaporthe grisea*. *Genes Dev* **10:** 2696–2706

Yu JH (2006) Heterotrimeric G protein signaling and RGSs in *Aspergillus nidulans*. *J Microbiol* **44:** 145–154

Yu JH, Wieser J, Adams TH (1996) The *Aspergillus* FlbA RGS domain protein antagonizes G protein signaling to block proliferation and allow development. *EMBO J* **15:** 5184–5190

Zheng B, Ma YC, Ostrom RS, Lavoie C, Gill GN, Insel PA, Huang XY, Farquhar MG (2001) RGS-PX1, a GAP for GalphaS and sorting nexin in vesicular trafficking. *Science* **294:** 1939–1942

